Structure-Based Design of Selective Histone Deacetylase 6 Zinc Binding Groups

Leandro A. Alves Avelar, Dusan Ruzic, Nemanja Djokovic, Thomas Kurz & Katarina Nikolic

Accepted author version posted online: 05 Aug 2019.

Submit your article to this journal ⬀

View Crossmark data ⬀

Structure-Based Design of Selective Histone Deacetylase 6 Zinc Binding Groups

Leandro A. Alves Avelar[1,2 #], Dusan Ruzic[2], Nemanja Djokovic[2], Thomas Kurz[1], and *Katarina Nikolic[2 #]*

[1]Institut für Pharmazeutische und Medizinische Chemie, Heinrich-Heine-Universität Düsseldorf, Universitätsstr. 1, 40225 Düsseldorf, Germany.

[2]Department of Pharmaceutical Chemistry, Faculty of Pharmacy, University of Belgrade, Vojvode Stepe 450, 11000 Belgrade, Serbia.

[#] LA and NK share corresponding authorship.

List of abbreviations: Area under curve, AUC; Autodock 4.2, AD4.2, benzohydroxamic acid, BHA; catalytic domain, CD; ChemScore Fitness Function, CSFF; fragment library, FL; hydroxamic acid, HA; hydrogen bond acceptor, HBA; histone deacetylase, HDAC; hydrogen bond donor, HBD; heat shock protein 90, Hsp90; molecular interaction field, MIF; Nexturastat A, NextA; pan assay interference substances, PAINS; protein data bank, PDB; Lipinski rule of three, Ro3; receiver operating characteristic, ROC; structure-based drug design (SBDD), structure-based virtual screening, SBVS, trifluoromethyloxadiazole, TFMO; ubiquitin proteasome system, UPS; zinc binding group, ZBG.

Abstract

The binding site of the second catalytic domain of human histone deacetylase 6 (HDAC6 CDII) has structural features that differ from the other human orthologues, being also mainly responsible for the overall enzymatic activity of this isoform. Aiming to identify new fragments as a possible novel selective zinc binding group (ZBG) for HDAC6 CDII, two fragment libraries were designed: one library consisting of known chelators and a second one using the fragments of the ZINC15 database. The most promising fragments identified in a structure-based virtual screening of designed libraries were further evaluated through molecular docking and molecular dynamics

simulations. An interesting benzimidazole fragment was selected from the *in silico* studies and presented as potential zing binding group for the development of novel HDAC6 selective inhibitors.

Introduction

Epigenetic alterations such as DNA methylation and post-translational histone acetylation are the most prevalent alterations of the genome. Histone Deacetylases (HDAC) are essential in this process and therefore attractive biological targets(Pande 2016). Eleven zinc-dependent HDACs isoforms are expressed in humans, sharing a highly conserved catalytic domain(de Ruijter et al. 2003). Among them, HDAC6 plays a key role in a wide range of diseases, due to its unique structural features and physiological functions (Batchu, Brijmohan, and Advani 2016). This histone deacetylase is a major α-tubulin and cortactin deacetylase and therefore playing a crucial role in the cytoskeletal dynamics affecting the cellular shape, division, transport, and migration (Kalin and Bergman 2013; Batchu, Brijmohan, and Advani 2016). The heat shock protein 90 (Hsp90) is also a substrate of HDAC6 and due to this interactions, HDAC6 is being associated with the removal of misfolded proteins trough the ubiquitin (Ub)-proteasome system (UPS) (Seidel et al. 2015).

The chemical structure of known HDAC inhibitors (HDACi) is composed of three different moieties: a cap group which interacts with the surface of the binding pocket, a linker (which can be aliphatic or aromatic) and a zinc binding group (ZBG). Although hydroxamic acids (HA) are the dominant class of ZBG, they do not show isoform selectivity(Roche and Bertrand 2016), in contrast to other moieties such as 2-aminobenzamides (HDAC1, 2 and 3 selective) (Bressi et al. 2010), 5-trifluoromethyl-[1 ,2,4] oxadiazole (HDAC4, 5, 7 and 9) (Murray-Thompson et al. 2013), 3-hydroxypyridin-2-thione (HDAC6 and 8) (Patil et al. 2013) and more recently benzoisothiazole (HDAC6) (Wu et al. 2017).

Recently the crystal structure of human HDAC6 catalytic domain II revealed a wide solvent exposed binding site flanked by a basin, believed to influence the substrate recognition. The wider binding site and presence of the basin are structural features, which can be used to design HDAC6 selective inhibitors. (Hai and Christianson 2016) Indeed, HDAC6-selective histone deacetylase inhibitors have already entered clinical trials against Multiple myeloma (Yang et al. 2017). The major part of these inhibitors contains a hydroxamic acid moiety as ZBG and their isoform selectivity is highly dependent on the inclusion of bulky cap groups and/or presence of an aromatic linker, which normally leads a Y-shaped binding conformation during the interaction with

HDAC6-binding site.(X. X. Wang, Wan, and Liu 2018; Liang and Fang 2018) Despite the success of hydroxamic acids as HDAC6-selective inhibitors, in some cases, hydroxamates are being quickly removed from the plasma by esterase-catalyzed hydrolysis and glucuronidation (Hermant et al. 2017). In addition to that, another limitation of this class of ZBG is their potential to undergo rearrangement to isocyanates in physiological conditions (Shen and Kozikowski 2016).

Structure-based drug design (SBDD) strategies have been successfully used in different aspects of the development of HDACi. Through the use of molecular dockings-based virtual-screenings allied to molecular s dynamics (MD), recent works discussed and proposed new chemical entities with improved selectivity towards different HDAC isoforms such as: HDAC1(Uba and Yelekçi 2018; Sixto-López, Bello, and Correa-Basurto 2019a), HDAC2 (Uba and Yelekçi 2018), HDAC3 (Uba and Yelekçi 2018; Amin et al. 2019), HDAC6 (Sixto-López, Bello, and Correa-Basurto 2019b), HDAC7 (Yuan et al. 2018), HDAC8 (Uba and Yelekçi 2018; Zhou et al. 2018; Kashyap and Kakkar 2019) and HDAC10 (Ibrahim Uba and Yelekçi 2019). Similar approaches showed also promising results when applied in design of dual-inhibitors (Y. Wang et al. 2019) as well as in the evaluation of protein-protein complexes involving HDAC8 (Mahalakshmi, Husayn Ahmed, and Mahadevan 2018).

Based on the success of the previous SBDD approaches in the design of HDACi, the aim of this study was to search for novel, chemically interesting fragments which physico-chemical properties as potential novel HDAC6 selective ZBGs.

Materials and Methods

Design of the Fragment Libraries

The initial step was the construction of the libraries FL1 and FL2. FL1 was created as a focused set of known metal binding fragments and consisted of the structures described in the works of Jacobsen et al. (Jacobsen et al. 2011), Chen et al. (Chen, Xu, and Wiest 2013) and from a chelator fragment library provided by Otava (Otava Chemicals 2017), in a total of 1021 entities. These 1021 molecules were then filtered using the Rule of 3 of Lipinski (Ro3) (Congreve et al. 2003) utilizing the software Instant JChem v17.3.27.0 (Chem Axon 2017a), the structures who passed this filter were then used as input for the FAF-drugs filtering tool (Lagorce et al. 2015). This second filtering step aimed to remove known toxicophores, possible aggregators and pan assay interference

substances (PAINS). Finally, fragments containing ZBGs present in known HDAC inhibitors (Roche and Bertrand 2016) were removed, resulting in the first library FL1 containing 268 fragments.

Contrarily to FL1, FL2 was designed to approach a broader spectrum of the chemical space, using the fragment collection of the ZINC15 database (Irwin et al. 2012). To build the second library, the tranches of ZINC15 containing substances with MW $\leq$ 200 and logP $\leq$ 3.0 were selected in a total of 499.688 compounds. This initial set of compounds was then further filtered using a modified Ro3 (HBD and HBA $\leq$ 3, rotatable bonds $\leq$ 3, asymmetrical atoms $\leq$ 1, number of rings $\leq$ 2), followed by the FAF-drug filter and the removal of known HDAC-ZBGs, resulting in a set of 183.223 fragments. Due to the size of the set, an additional filter was applied using the software FLAP in the bit-string mode (Baroni et al. 2007). In the bit-string mode the binding site of human HDAC6-CDII (PDB 5EDU) was used as template for measure of quadruplets similarity between binding site and ligands, without generation of GRID fields (Goodford 1985). The pre-filtered compounds were ranked according to complementarity to the probes of the template through the sum of the combinations of all probes (Global Sum).(Goracci et al. 2016) Fragments with values > 400 were selected in a total of 1501 compounds forming FL2.
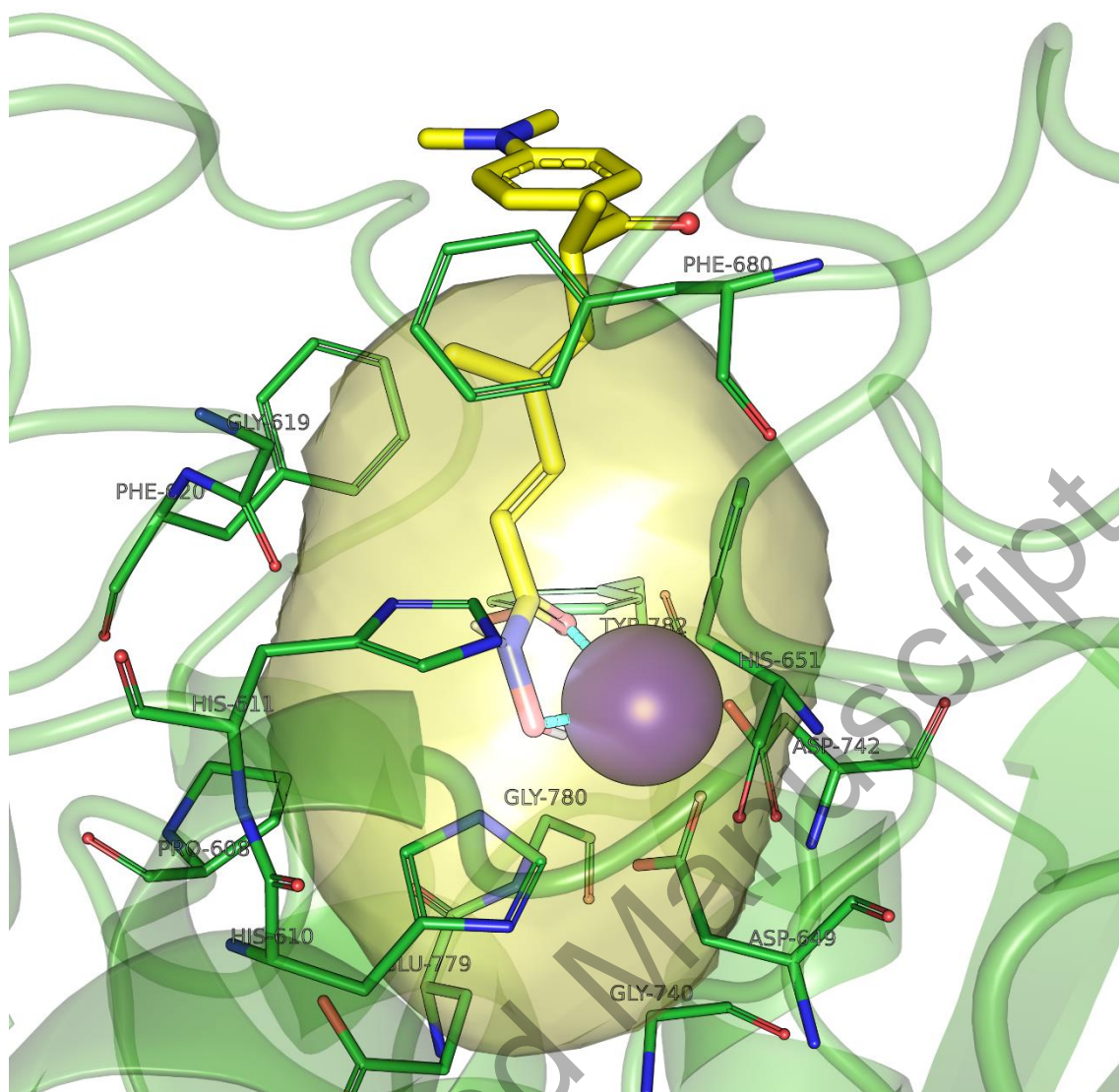
Figure 1: Human histone deacetylase 6 (second catalytic domain) complexed with Trichostatin A (PDB 5EDU); region of the HDAC6-CDII (Hai and Christianson 2016) in yellow defined as the template for the pre-screening (zinc atom in grey).

Validation of structure-based HDAC6 virtual screening model

In order to evaluate the quality of the virtual screening model a set of active and a set of inactive fragments were built using the Chembl database (Gaulton et al. 2017), molecules with MW ≤ 250 containing IC_{50} values for HDAC6 were searched and 30 selected (KrennHrubec et al. 2007; P. Jones et al. 2008; Mazitschek et al. 2008; Kemp et al. 2011; Fass et al. 2011; Bürli et al. 2013; VanHeyst et al. 2013; Patil et al. 2013; Olson et al. 2013; Wagner et al. 2013; Giannini et al. 2014; Muthyala et al. 2015; Wu et al. 2017) (Table S1, ESI). The fragments with IC_{50} >10 uM were defined as inactive in the screening (10 fragments), while the fragments with IC_{50}<7.5 µM were defined as

active (20 fragments) fragments with IC_{50} values $\leq$ 10 uM and $\geq$ 7.5 μM were set as undefined and were not included in the validation data set. A total of 20 fragments were defined as active and 10 as inactive and no fragment was defined as undefined (Table S1, ESI).

Structure-based virtual screening

The crystal structure of the second catalytic domain of the human HDAC6 PDB 5EDU (Hai and Christianson 2016) was used as the target, enabling the presence of the zinc atom in the calculation of the MIFs. The screenings were performed in the high accuracy mode and the combination of GRID probes ranked by the AUC of their ROC plot.

FL1 and FL2 were used as input for the software FLAP, where for each fragment molecular interaction fields – (MIF) were calculated by use of GRID probes (DRY, O, N1 and H). Hydrophobic (DRY) probe and hydrogen bond regions (O probe identifies hydrogen bond donating group, whereas N1 probe identifies hydrogen bond accepting group of the screened fragments) described along with molecular shape (H probe) were extracted in quadruplets of pharmacophoric points. The template used for SBVS was the MIF derived pharmacophore calculated within 2.5 Å of the zinc ion present in the active pocket of HDAC6 isoform (Perruccio et al. 2006).

Once the molecular interaction field (MIF) with the minimum energy is calculated within the active site, the pharmacophoric feature of the target protein is stored as a template. MIF quadruplets which belong to the active pocket of the protein are further superimposed with the quadruplets of the screened compounds. The quantification of the pharmacophoric superimposition between tested ligands and pharmacophore of the active pocket is evaluated by the calculation of probe scores. The screened compounds could be ranked according to 19 different scores with regard to the pharmacophore of the template (Cruciani 2006).

Molecular docking

The fragments were docked in the crystal structures of HDAC1 PDB 5ICN (Watson et al. 2016), HDAC 4 PDB 4CBY (Bürli et al. 2013), HDAC6-CDII PDB 5EDU (Hai and Christianson 2016) and HDAC8 PDB 3SFF (Whitehead et al. 2011) using the software GOLD v5.6 (G. Jones et al. 1997) and Autodock 4.2 (AD4.2) (Morris et al. 1998). The

receptors were prepared by removing all the water molecules and ions with the exception of the catalytic zinc, followed by the addition of polar hydrogens of the amino acids in Discovery Studio v. 17.2.0 (Dassault Systèmes BIOVIA 2016). Additionally, the missing atoms and the protonation of the ionizable amino acid residues was accomplished by use of the Play Molecule web-server (Martínez-Rosell, Giorgino, and De Fabritiis 2017). Ligands were prepared in ChemDraw 3D v15.0 (PerkinElmer 2015) software, whereas the minimization of their structures was performed using the MM2 method implemented in Gaussian software (M.J. Frisch, G.W. Trucks, H.B. Schlegel, G.E. Scuseria, M.A. Robb, J.R. Cheeseman, G. Scalmani, V. Barone, B. Mennucci, G.A. Petersson, H. Nakatsuji, M. Caricato, X. Li, H.P. Hratchian, A.F. Izmaylov, J. Bloino, G. Zheng, J.L. Sonnenberg, M. Hada, M. Ehar 2009). Protonation of the fragments was defined at $pH = 7.4$ in Marvin Sketch v17.27 (Chem Axon 2017b). For the dockings using Autodock 4.2, the clean structures of the proteins and the minimized structures of the ligands were prepared using the standard procedure of AutoDock tools version1.5.7 (Morris et al. 1998).

For the docking studies in GOLD v5.6, the binding site of the respective HDACs was defined as those amino acids in 8 Å within the zinc atom, the parameters were defined as 30 generic algorithm runs with 100 poses, clustered in 6 resolutions. To estimate the binding affinity of the studied fragment-HDAC complexes, ChemScore fitness function (CSFF) (Eldridge et al. 1997) was used. Root-Mean-Square Deviation (RMSD) values between co-crystal ligands and their docked conformations in ligand-HDAC complexes were calculated to ensure that the docking procedure is valid and accurate for further predictions (Table S2, ESI). Finally, the CSFF values were used to select the most promising HDAC6 selective fragments. The main objective was to extract those fragments with the highest values of CSFF calculated for the certain fragment-HDAC6 interactions. Additional criteria used for discriminating possible non-selective ligands were the pose and the orientation of the studied fragments inside the active pockets of studied HDACs.

In the dockings performed in AD4.2, for each enzyme, a grid box with size 15 x 15 x 15 with the spacing of 1.0 Å centered in the cocrystalized ligand was created and the Lamarckian genetic algorithm of AD4.2 was used. The search parameters were set to 100 GA runs for each ligand with a population size of 150, maximum number of 2.5 $x10^6$ energy evaluations with a maximum number of 2.7 104 generations, a mutation

rate of 0.2 and a crossover rate of 0.8 and the default dockings parameters were used. Populations of 100 docking poses were generated and the first pose of the cluster containing minimum of one interaction between oxygen, nitrogen or sulfur with the catalytic zinc (distance of heteroatom and zinc ion >3.0 Å) was chosen, whether no such interaction was observed, the first pose of the lowest energy cluster was used. Similarly, to the dockings performed with GOLD, the validation of the docking protocols was performed trough redocking studies (Table S2, ESI).

Molecular Dynamics

In order to study binding stability of HDAC6-ligand complexes and to refine binding modes obtained through molecular docking, short molecular dynamics (MD) simulations were performed. MD simulations were performed using Groningen Machine for Chemical Simulation (GROMACS v5.1.5) software (Pronk et al. 2013). All simulated complexes were obtained through molecular docking. The AMBER99SB-ILDN force field (Lindorff-Larsen et al. 2010) was used for generation of protein topology, while ligand parameters were derived from General Amber force field (GAFF2) (Vassetti, Pagliai, and Procacci 2019), with calculation of RESP atomic charges using HF-6-31G* basis set. Force field parameters for all ligands were assigned using the AnteChamber Python Parser interfacE (ACPYPE) (Sousa da Silva and Vranken 2012). The protein-ligand complexes were solvated with TIP3P water model, and neutralized with Na^+ counterions in octahedral periodic box. Potassium ions from PDB: 5EDU were kept. Systems were minimized with steepest descent algorithm with maximum force set to 10 kJ mol^{-1} nm^{-1} and 5000 steps. Subsequent equilibration of the systems was performed firstly in NVT ensamble for 100 ps at 310 K using V-rescale thermostat, secondly in NPT ensamble for 100ps maintaining the preasure at 1.0 bar with Parrinello-Rahman barostat. All atom position restrains were applied on protein atoms, while the solvent molecules and counterions were unrestrained. 20 ns of production runs were performed for each complex at constant temperature (310 K) and pressure (1 bar) using Particle Mesh Ewald (PME) approach for calculation of long-range electrostatic interactions using a 10 Å cut-off value. LINCS alghorithm was used for all bonds constrains, including H atoms. Obtained trajectories were analysed using Gromacs built-in *gmx_rms* and *gmx_rmsf* tools.

Binding free energy calculation

The binding free energies of protein-ligand complexes were estimated with Poison-Boltzmann surface area (MM/PBSA) method implemented in GMXPBSA 2.1 (Paissoni et al. 2015) software. Calculation was performed on ensemble of structures extracted in last 5 ns of trajectories, after removal of solvent molecules and cations, except zinc. Briefly, the binding free energy of a protein molecule to a ligand molecule in solution is defined as:

$$\Delta G_{binding} = G_{complex} - \left(G_{protein} + G_{ligand}\right) \tag{1}$$

where free energy term is calculated from thermodynamically weighted ensemble of structures as follows:

$$\langle G \rangle = \langle E_{MM} \rangle + \langle G_{solv} \rangle - T \langle S_{MM} \rangle. \tag{2}$$

The energetic term E_{MM} is defined as:

$$E_{MM} = E_{int} + E_{coul} + E_{LJ} \tag{3}$$

where E_{int} indicates bonded (bond, angle, and torsional angle energies), and E_{coul} and E_{LJ} represents nonbonded interactions (intramolecular electrostatic and Lennard-Jones energies) calculated based on molecular mechanics (MM) force-field parameters. The free energy of solvation (G_{solv}) in Eq. (2) is the energy required to transfer a solute from vacuum into the solvent and it is calculated as sum of polar (G_{polar}) and nonpolar solvation energies ($G_{nonpolar}$).

$$G_{solv} = G_{polar} + G_{nonpolar} \tag{4}$$

G_{polar} is calculated based on Poisson-Boltzmann equation and represents energy required to transfer the solute from continuum medium with a low dielectric constant ($\varepsilon = 1$) to a continuum medium with dielectric constant of water ($\varepsilon = 80$). The nonpolar solvation energy includes repulsive and attractive forces between solute and solvent that are generated by cavity formation and van der Waals interactions and it can be aproximated to be proportional to solvent accessible surface area (SASA):

$$G_{nonpolar} = \gamma SASA + \beta \tag{5}$$

Where $\gamma = 0.0227$ kJ mol^{-1}Å^{-2} and $\beta = 0$ kJ mol^{-1}.

Entropy contribution ($T \langle S_{MM} \rangle$ in Eq. (2)) was neglected because calculation of entropy contribution is time-consuming process and it can be cause of larger error of prediction

(Homeyer and Gohlke 2012). Calculated energies were used as scores for relative comparison of binding affinities between structurally related ligands.

Results and Discussion

Virtual screenings

In the validation of virtual screening protocol, two FLAP scores (H*N1 and H*N1*H) performed the best in discriminating known active and inactive fragments with the AUC values of 0.84. The ROC curves with enrichment factors are presented in Figure 3. The H*N1 score indicates that screened ligands should match the shape (Figure 2, blue mesh) and hydrogen bond accepting interactions (blue surface) within the active pocket of HDAC6 (CD II).
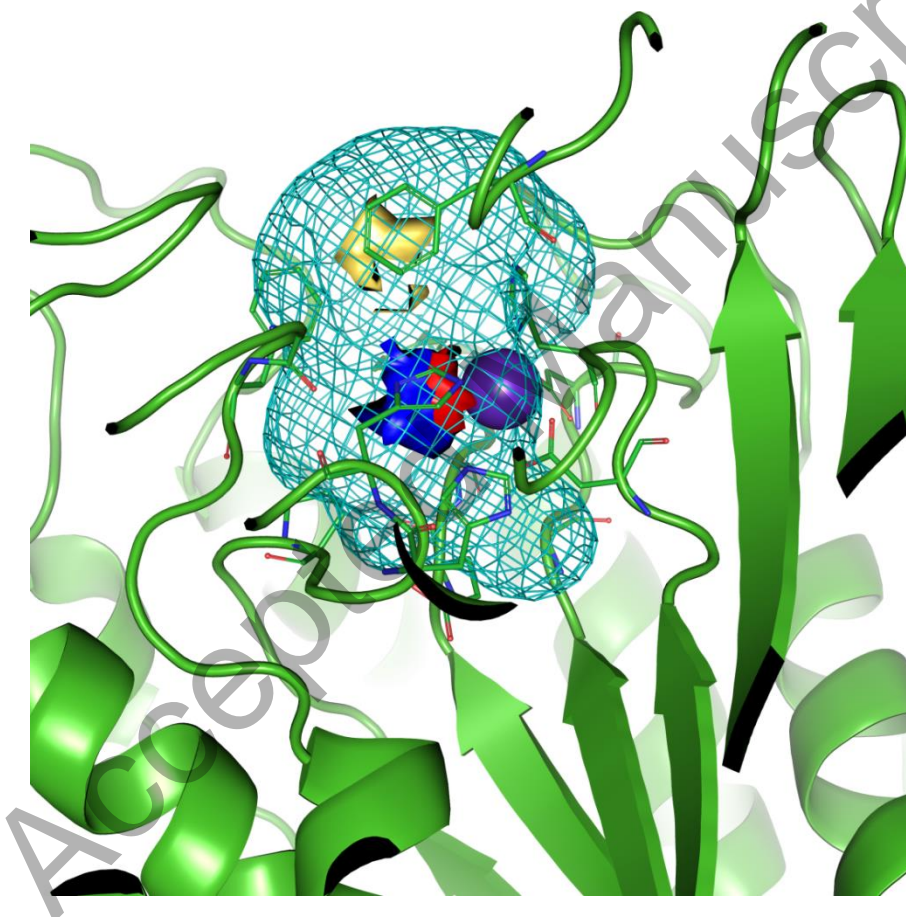

Figure 2: Representation of the MIFs calculated for defined ZBG binding site in HDAC6-CDII (PDB 5EDU): H probe (blue mesh surface), O1 (red surface), N1 (blue surface), and DRY (yellow surface) zinc atom showed as a purple sphere).

For the virtual screening of smaller FL1 database (268 fragments), the product of the shape (H) and hydrogen bond donor (N1) probes (H*N1) was used as the score for

identifying the fragments which pharmacophore is closely overlapping with the pharmacophore of the template (Figure 3). As it can be observed from Figure 3 this probe score performed slightly better in classification of first 10% of assayed fragments, which makes it more suitable for smaller FL1 database compared to H*N1*H score which performed better for larger database (FL2). At 1% of false positive fragments, 32% true active fragments were recovered. Conclusively, if 5% of the top-ranked fragments were assayed, 74% of them would have shown affinity toward HDAC6 isoform.
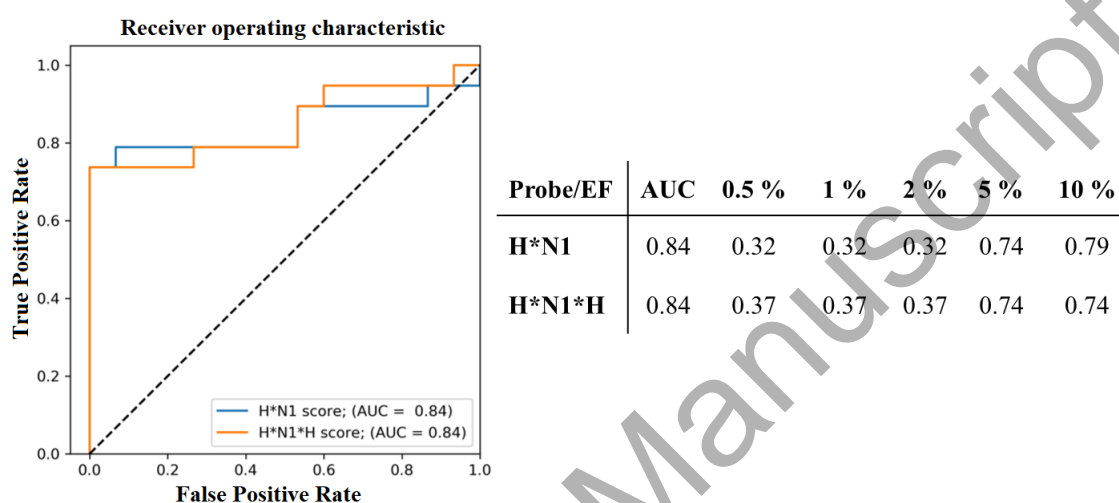

Probe/EF	AUC	0.5 %	1 %	2 %	5 %	10 %
H*N1	0.84	0.32	0.32	0.32	0.74	0.79
H*N1*H	0.84	0.37	0.37	0.37	0.74	0.74

Figure 3: Results of validation of the virtual screening models performed using FL1 (blue line) and FL2 (orange line)

Structure-based virtual screening model used for the screening of FL2 database gave a good enrichment with AUC of 0.84, where the overlaps of different shapes (H) and hydrogen bond donor (N1) molecular interaction fields determined the highest ranking of the active fragments in the first 5% of false positive fragments (Figure 3). When SBVS was performed with the FL2 database, the highest performance of the virtual screening was achieved by ranking the compounds according to the H*N1*H probe score. This probe score defines good overlapping between hydrogen bond acceptor group and shape properties of the screened fragments with the pharmacophore features defined in the HDAC6 pocket around Zn^{2+} ion.

In each of both SBVS protocols, the compounds were ranked according to the selected probe and the 20 top-ranked fragments were selected for the docking studies (Table S3 and S4, ESI) in a total of 40 fragments.

Molecular docking

The chosen 40 fragments were docked in the structures of four HDACs (HDAC1, 4, 6 and 8) representing the different subclasses I, IIa and IIb. HDAC1 belongs to class I and it is known to have high homology to HDAC2 and HDAC3. HDAC1, however, presents a lower degree of identity to HDAC8, which have been shown to have unique architecture among this class (Wagner et al. 2016) and was therefore also used in the dockings studies. HDAC11, the sole representative of class IV HDAC up till now has no crystal structure and due to its similarity with HDAC8 (Kutil et al. 2017) was not used in this study.

In each docking, the poses with the highest CSFF values were selected and visually analyzed in regards to its coordination with the zinc ion using the software Discovery Studio Visualizer Software v17.2 (Dassault Systèmes BIOVIA 2016). The scores of the best poses of the selected fragments are shown in Table S5. In addition to the fragments, benzohydroxamic acid (BHA) was also docked using the same protocol, BHA was chosen for the dockings due to its preference towards HDAC6 and due to the availability of IC_{50} values (HDAC1 4.73 μM, HDAC4 >33.3 μM, HDAC6 0.11 μM, and HDAC8 1.92 μM) (Wagner et al. 2013) and Ki values (HDAC6 0.114 μM, and HDAC8 3.00 μM) (Porter, Wagner, and Christianson 2018) for the evaluated isoforms.

The metal-binding geometry and interaction distances between small molecules and metalloproteins stand as a challenging subject (Martin et al. 2014; Cohen 2017), to approach it, Kawai et al (Kawai and Nagata 2012) used the crystal structures of the metalloproteins containing zinc present in the PDB to determinate the average distance between the ZBG and the nearest ligand atoms. It was observed that only nitrogen, oxygen, and sulfur interacted with the zinc ion with average distances of 1.99, 2.05 and 2.28 Å (with a variation of ± 0.1 Å) respectively. Also, it was shown that the distance between the second heteroatom to interact with the zinc in bidentate ZBGs occurs in a wide range of distances, not being well defined. Metal binding groups can also act via non-chelating interactions with the zinc ion. The trifluoromethyloxadiazole (TFMO) is the ZBG of a known group of class IIa selective HDACi and interacts with the ion through one of its fluorine and the oxygen of the oxadiazole ring in a distance of 2.7 and 3.0 (Å) respectively (Murray-Thompson et al. 2013).

Among the 40 fragments, thirty of them were predicted to interact with the Zn^{2+} ion inside the catalytic site of HDAC6 (CD2). The fragments were selected by comparing the CSFF values calculated for BHA after docking on HDAC6 isoform. Only those fragments which showed higher CSFF than BHA (**3, 4, 13** and **16**) were selected for further studies (Figure 4). Additionally, the pose and orientation of the selected fragments were examined. ChemScore fitness function for fragment **7** was 36.5756, which is significantly higher than for BHA (31.6326). CSFF value for HDAC8 docking procedure (36.8017) was close to the score obtained for HDAC6 docking, making this fragment potentially promiscuous for further studies.
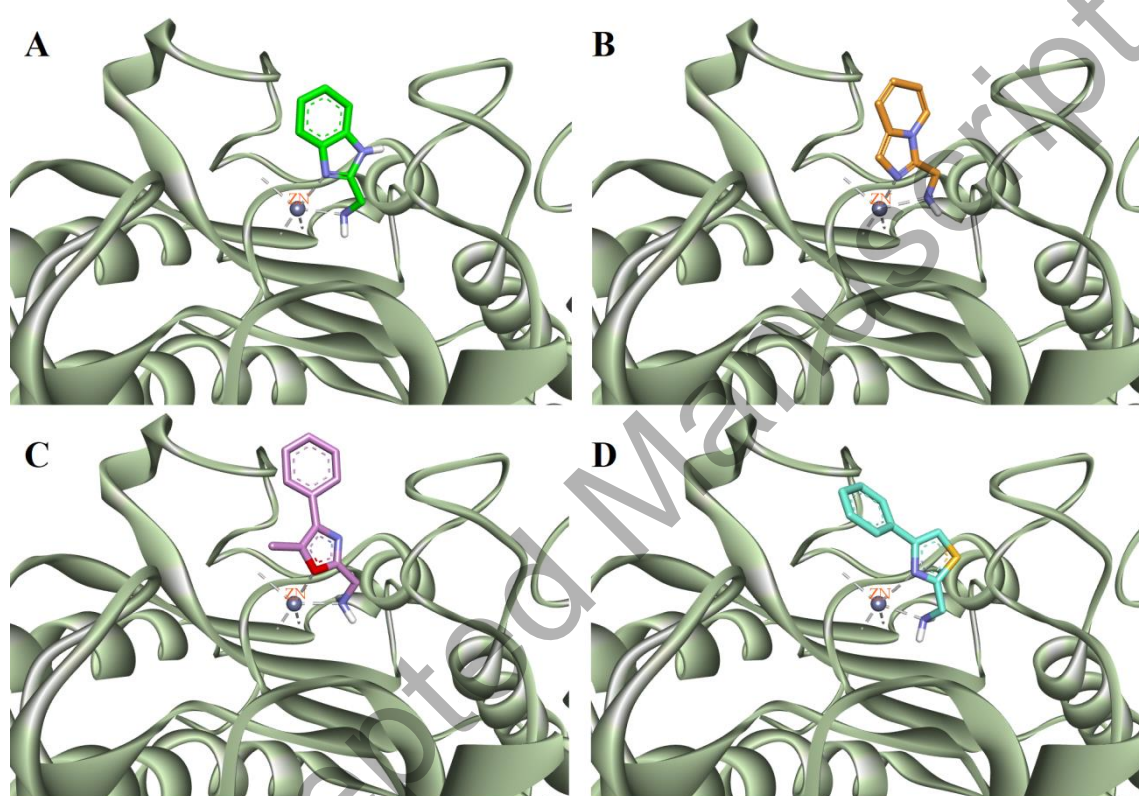

Figure 4. Initial poses of the best selected fragments obtained after molecular docking study in CDII of HDAC6; A) fragment **3**, B) Fragment **4**, C) Fragment **13** and D) Fragment 16.

In general, better *in silico* selectivity profile was achieved among first 20 fragments (FL1 database) with aromatic or heterocyclic zinc binding groups, whereas the aliphatic ZBG extracted from the second screening (FL2 database) were inferior despite their relative smaller size, what could be due to the higher flexibility of these fragments.

The denticity of HDACi inhibitors was recently related to the nature of their selectivity towards HDAC6 (Porter et al. 2017, 2018; Porter, Wagner, and Christianson 2018), short-linker hydroxamic acids with bulky cap-groups are known to present high

selectivity towards HDAC6. Due to steric hindrance, the hydroxamate of these inhibitors binds as a monodentate ligand. Although energetically less favorable than bidentate interactions, this binding does not compromise the affinity of these compounds (KrennHrubec et al. 2007). Molecular docking study in GOLD software showed that fragments **3**, **4**, **13** and **16** coordinate to Zn^{2+} ion in bidentate fashion inside HDAC6 (Figure S3, ESI). To the respect of the results obtained after molecular docking study, we subjected selected fragments to the molecular dynamic simulations in order to access the stability of the predicted binding modes.

Contrary to the dockings performed using GOLD, in the docking performed with AD4.2 the *in silico* selectivity of BHA was correctly predicted, with higher binding energies being observed for HDAC6, followed by HDAC1, HDAC4 and HDAC8 (Table S5, ESI). Similarly, to the first dockings studies, using AD4.2 15 fragments showed better scores for HDAC6 than the other isoforms, with 10 fragments having preference for HDAC1, two for HDAC4 and 3 for HDAC8. Interestingly, the fragments containing carboxylic acids (**1**, **2**, **6**, and **20**) presented higher docking energies than BHA, a behavior that contradicts experimental data, once carboxylic acids are known to be limited to weak inhibition of HDACs (Roche and Bertrand 2016).

Despite the correct prediction of BHA *in silico* selectivity, in the dockings using AD4.2 (Table S5, ESI) a total of 10 fragments (**8, 11, 13, 16, 24, 25, 30, 33, 39** and **40**) showed no interaction between fragment and the catalytic zinc. These fragments, although not showing interactions with the catalytic zinc, showed similar dockings energies to other fragments with both mono- and bidentate ligands. Therefore, the selection of the fragments for the molecular dynamic studies was based on the docking results performed with the software GOLD.

In order to further analyze binding stability of fragments **3**, **4**, **13** and **16**, short molecular dynamics runs were performed. The obtained docking poses of fragments **3**, **4**, **13** and **16** showed stable root-mean-square deviations (RMSD) for Cα atoms (Figure 5) through 20 ns of simulations indicating the overall stability of protein-ligand complexes. RMSD plots calculated for fragment atoms are shown in Figure S5 in the ESI. Obtained RMSD plots also indicates overall stability of protein-fragment interaction patterns obtained through molecular docking, further validating our docking protocol. MM/PBSA calculations were performed on last 5 ns of each trajectory in order to ensure convergence of simulations. Calculated MM/PBSA scores indicate

favorable predicted binding energies of identified fragments where fragment **3** was the most promising candidate for further evaluation which is in accordance to molecular docking prediction (Table 1). Calculated polar contribution of binding free energy for fragments **13** and **16** was unfavorable for binding, indicated that electrostatic interaction, as favorable component of polar contribution was not enough for overcoming larger polar solvation barrier. This was not case for fragments **3** and **4**. Nonpolar contribution was the major driving force of binding for fragments **4**, **13** and **16** where Van der Walls interaction energies, as the component of total nonpolar contribution, had the more significant effect on total binding energy. In the case of fragment **3**, polar contribution was the major driving force.

According to previous research in the field of novel ZBGs for HDACs, 2-(aminomethyl)pyridines were predicted to be promising zinc-binding groups for HDACs in quantum mechanics calculations (Chen, Xu, and Wiest 2013). Further, few HDAC8 selective and potent inhibitors with alpha-amino carbonyl moiety as zinc binding group were described previously (Whitehead et al. 2011) and X-ray structures (PDB IDs 3SFF and 3SFH) revealed that unionized amino group is responsible for coordination, while carbonyl group interact with zinc through weakened electrostatic interactions. Above mentioned data further justify our results. In order to provide additional validation of our results pKa values were calculated for alpha-amino carbonyl HDAC8 inhibitor and fragment **3**. Furthermore, binding modes of HDAC8-amine complex (PDB ID 3SFF) and predicted HDAC6-fragment **3** complex were compared. Predicted pKa values of fragment **3** and known HDAC8 inhibitor (from PDB ID 3SFF) using *cxcalc* tool from Chem Axon (Chem Axon 2017b) for ligands alone (pKa $_{pred}$ (fragment **3**) = 7.90; pKa $_{pred}$ (pdb 3SFF) = 7.92), and PROPKA 3.1 (Søndergaard et al. 2011) for protein-ligand complexes (pKa $_{pred}$ (fragment **3**) = 7.99; pKa $_{pred}$ (pdb 3SFF) = 8.55) are in agreement, further justifying fragment **3** as novel zinc-binding group. In the Figure S6 superposition of known HDAC8-amine inhibitor complex with docked pose of fragment **3** in HDAC6 is presented.
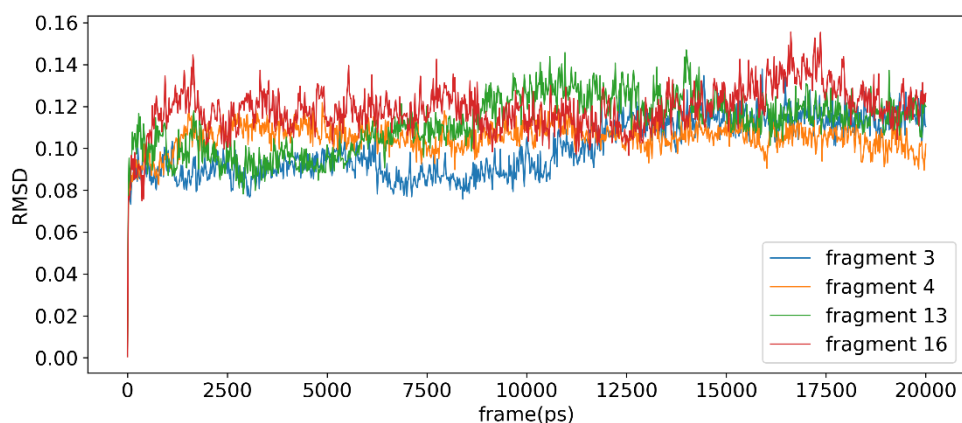
Figure 5. Root-mean-square deviations (RMSD) of Cα atoms calculated for 20 ns of MD simulation.

Root mean square fluctuation (RMSF) analysis for all fragments complexes simulated indicates no significant deviations from fluctuations of residues observed for apo-protein MD simulations (Figure S7, ESI). Interestingly, residues 550-565 placed in close proximity of cap-group binding site were the most fluctuating part of HDAC6 during all MD simulations (Figure S7 and S8, ESI).

Table 1. Binding-free energies for protein–ligand complexes calculated with MM/PBSA method for the MD simulations (kJ/mol).

Computation					
	Polar contribution		Nonpolar contribution		
	ΔE_{coul}	ΔG_{polar}	ΔE_{vdW}	$\Delta G_{nonpolar}$	$\Delta G_{binding}$
fragment **3**	-341.709	296.416	-24.680	-9.666	-79.639
fragment **4**	-317,787	303,585	-23,123	-10,039	-47,364
fragment **13**	-232,229	262,779	-45,305	-12,659	-27,414
fragment **16**	-242,867	262,618	-53,367	-11,390	-45,005
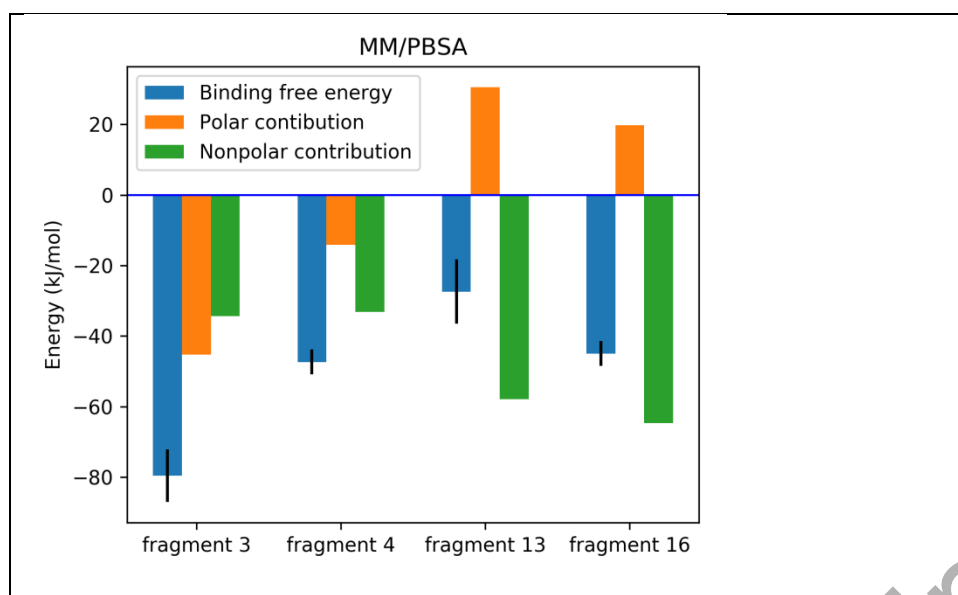
To further explore the application of molecular docking for the identification of HDAC6 selective fragments and to rationalize the results observed in the dockings of BHA, additional docking studies were performed using Nexturastat A (NextA) and compound **41** (Figure 4). NextA is a BHA-based HDACi with more than 600-fold selectivity towards HDAC6 over HDAC1 (Bergman et al. 2012), despite the presence of the BHA as selective ZBG, the selectivity of NextA have been also related to the shape and interaction of its connecting unit and cap group (Figure 6) with the shallow binding site of HDAC6 (Hai and Christianson 2016; Porter et al. 2018). Therefore, the linker cap group of NextA were connected to fragment **3** to form the theoretical full inhibitor **41**. Fragment **3** was chosen because it showed the highest selectivity towards HDAC6 when compared to HDAC1 in the performed docking studies.
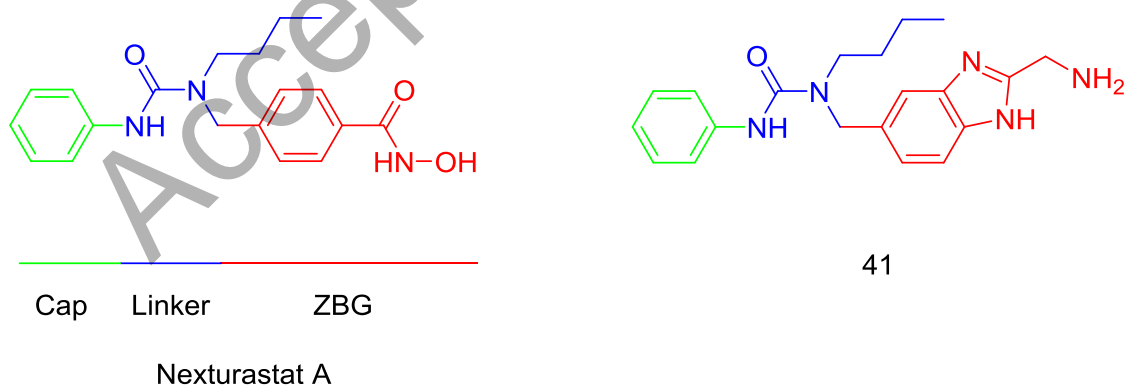

Figure 6: Structure of the classical pharmacophore of HDACi represented by Nexturastat A and the proposed structure of compound **41**.

Nexturastat A and compound **41** were docked in the crystal structures of HDAC6 and HDAC1 using the same protocols applied for the fragments. The docking energies of the highest poses are shown in Table 2.

Table 2: ChemScore Fitness Function (CSFF) values of NextA and compound **41**.

Compound	CSFF	
	HDAC6	HDAC1
Nexturast A	34,3581	32,2896
41	46,1364	33,8233

Unlike BHA, the docking energies of NextA were lower for HDAC6 than for HDAC1, which agrees with the experimental data. These results showed that the inclusion of the ZBG-fragment BHA in the complete pharmacophore of HDACi lead to a better correlation between docking energies and biological activity. A similar result was also observed for compound **41**. Compound **41** showed better scores in the docking with HDAC6 than HDAC1. In the docked poses of **41** in HDAC1 and HDAC6 (Figure S8 A) the ZBG showed interactions with the zinc ion through the free amino group of the methylamino group and with the non-alkylated imidazolic nitrogen. Despite the similarity observed in the zinc binding of **41** with both isoforms, due to the tighter hydrophobic channel of class I HDACs the cap group of the inhibitor suffers steric constraints (Figure S8 A), what could lead to low activity against this isoform. On the other hand, the shallower and wider binding site of HDAC6 has enough space to accommodate the cap group of **41** (Figure S8 B). Short MD run for both compounds have been performed and calculated MM/PBSA scores (Table S6, ESI) are in accordance with docking results (Table 2). After 20 ns of MD simulations both ligands retained binding modes similar to binding modes in starting complexes obtained through docking simulations (Figures S10 and S11). Comparison of binding modes after MD simulation for compounds **41** and NextA bounded to HDAC6 are presented on the Figure 7. Cap group of NextA retained in the same conformation as in HDAC6- ligand **41** complex indicating that fragment **3** could be suitable replacement for phenylhydroxamate ZBG.
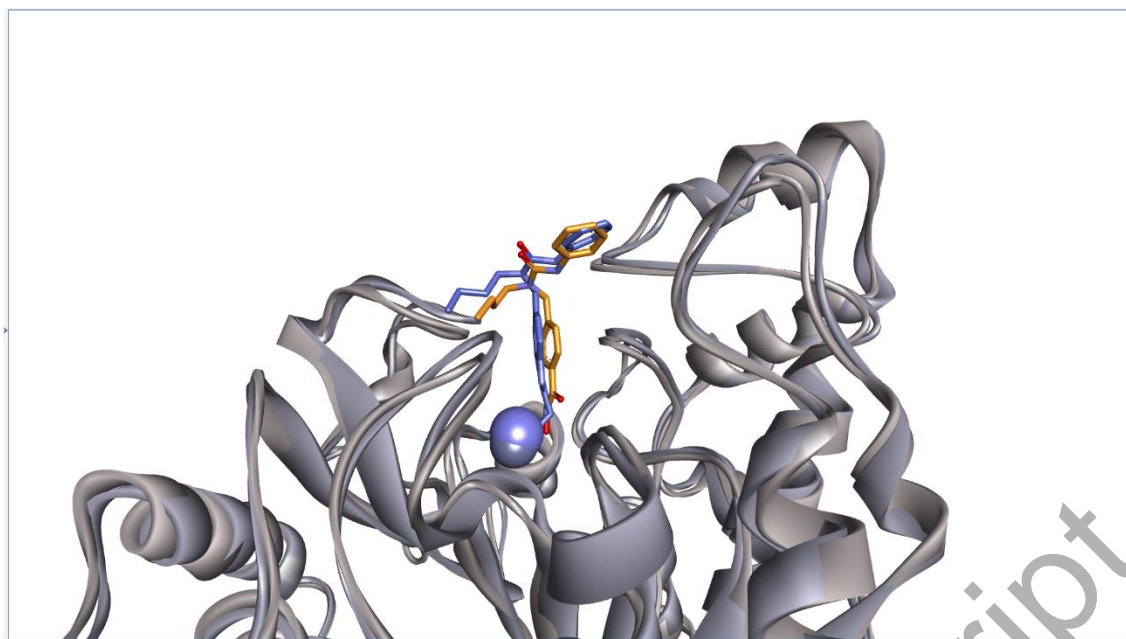
Figure 7. Comparison of binding modes of NextA (orange) and designed ligand 41 (blue) obtained through MD simulations. Protein-ligand complexes are extracted from converged parts of trajectories.

For several years HDAC6 has been used as a target for the design of selective inhibitors, however, the first crystal structures of this enzyme was only available since 2016 (Hai and Christianson 2016). Even before the first 3D structure was available, the use of homology models gave basis to structure-based drug-design in which selective HDAC6/8 ZBGs were identified (Patil et al. 2013). Also, HDAC6-selective non-hydroxamic inhibitors were identified via pharmacophore-based and structure-based virtual screenings using such models (Goracci et al. 2016). The deeper understand of the role of the ZBG in HDAC6 selectivity presented in more recent studies (Porter et al. 2017, 2018) lead to a positive impact in the silico design of HDAC6 inhibitors, whereas in more recent works the interactions of non-hydroxamic ZBG can be better rationalized (Sharma et al. 2019).

Conclusion

HDAC6 is involved in a wide myriad of physiological roles and despite the successful development of selective inhibitors for this isoform, so far, they are all restricted to hydroxamate-based structures. Different from other HDAC classes, up till now no selective ZBG have been validated for HDAC6. Aiming to propose a new fragment as novel HDAC6-ZBG, a combined strategy of SBVS and molecular docking was performed. The four most promising fragments identified had their interaction with

HDAC6 further evaluated using molecular dynamics to confirm the likelihood of their interaction with the targeted enzyme. A systematic *in silico* validation of this approach led to identification of fragment *(1H-Benzoimidazol-2-yl)-methylamine* as potential ZBG. Furthermore, a full inhibitor containing the structure of Fragment **3** was proposed and also evaluated in silico in terms of its isoform selectivity, showing to be a potential lead structure for the synthesis of new non-hydroxamic HDAC6-selective inhbitors.

Supplementary data

Tables S1-S6 and Figures S1-S11 are provided as supplementary information.

Acknowledgements

Conflicts of interest

The authors declare no conflict of interest.

References

Amin, Sk Abdul, Nilanjan Adhikari, Tarun Jha, and Balaram Ghosh. 2019. "Designing Potential HDAC3 Inhibitors to Improve Memory and Learning." *Journal of Biomolecular Structure and Dynamics* 37 (8): 2133–42. https://doi.org/10.1080/07391102.2018.1477625.

Baroni, Massimo, Gabriele Cruciani, Simone Sciabola, Francesca Perruccio, and Jonathan S. Mason. 2007. "A Common Reference Framework for Analyzing/Comparing Proteins and Ligands. Fingerprints for Ligands and Proteins (FLAP): Theory and Application." *Journal of Chemical Information and Modeling* 47 (2): 279–94. https://doi.org/10.1021/ci600253e.

Batchu, Sri N, Angela S Brijmohan, and Andrew Advani. 2016. "The Therapeutic Hope for HDAC6 Inhibitors in Malignancy and Chronic Disease." *Clinical Science (London, England : 1979)* 130 (12): 987–1003. https://doi.org/10.1042/CS20160084.

Bergman, Joel A., Karrune Woan, Patricio Perez-Villarroel, Alejandro Villagra,

Eduardo M. Sotomayor, and Alan P. Kozikowski. 2012. "Selective Histone Deacetylase 6 Inhibitors Bearing Substituted Urea Linkers Inhibit Melanoma Cell Growth." *Journal of Medicinal Chemistry* 55 (22): 9891–99. https://doi.org/10.1021/jm301098e.

Bressi, Jerome C., Andy J. Jennings, Robert Skene, Yiqin Wu, Robert Melkus, Ron De Jong, Shawn O'Connell, Charles E. Grimshaw, Marc Navre, and Anthony R. Gangloff. 2010. "Exploration of the HDAC2 Foot Pocket: Synthesis and SAR of Substituted N-(2-Aminophenyl)Benzamides." *Bioorganic and Medicinal Chemistry Letters* 20 (10): 3142–45. https://doi.org/10.1016/j.bmcl.2010.03.091.

Bürli, Roland W., Christopher A. Luckhurst, Omar Aziz, Kim L. Matthews, Dawn Yates, Kathy. A. Lyons, Maria Beconi, et al. 2013. "Design, Synthesis, and Biological Evaluation of Potent and Selective Class IIa Histone Deacetylase (HDAC) Inhibitors as a Potential Therapy for Huntington's Disease." *Journal of Medicinal Chemistry* 56 (24): 9934–54. https://doi.org/10.1021/jm4011884.

Chem Axon. 2017a. "Instant JChem V17.3.27.0." https://chemaxon.com/products/instant-jchem.

———. 2017b. "Marvin Sketch V17.27." https://chemaxon.com/products/marvin.

Chen, Kai, Liping Xu, and Olaf Wiest. 2013. "Computational Exploration of Zinc Binding Groups for HDAC Inhibition." *The Journal of Organic Chemistry* 78 (10): 5051–55. https://doi.org/10.1021/jo400406g.

Cohen, Seth M. 2017. "A Bioinorganic Approach to Fragment-Based Drug Discovery Targeting Metalloenzymes." *Accounts of Chemical Research* 50 (8): 2007–16. https://doi.org/10.1021/acs.accounts.7b00242.

Congreve, Miles, Robin Carr, Chris Murray, and Harren Jhoti. 2003. "A 'Rule of Three' for Fragment-Based Lead Discovery?" *Drug Discovery Today* 8 (19): 876–77. https://doi.org/10.1016/S1359-6446(03)02831-9.

Cruciani, Gabriele. 2006. *Molecular Interaction Fields : Applications in Drug Discovery and ADME Prediction*. Wiley-VCH. https://www.wiley.com/en-us/Molecular+Interaction+Fields%3A+Applications+in+Drug+Discovery+and+ADME+Prediction-p-9783527607136.

Dassault Systèmes BIOVIA. 2016. "Discovery Studio v.17.2.0." https://www.3dsbiovia.com/products/collaborative-science/biovia-discovery-studio/visualization-download.php.

Eldridge, Matthew D, Christopher W Murray, Timothy R Auton, Gaia V Paolini, and Roger P Mee. 1997. "JCAMD_1997_11_425_Eldridge" 11: 1–21. papers3://publication/uuid/EDB550EA-F218-4741-A298-02AF9CCB2D57.

Fass, Daniel M., Rishita Shah, Balaram Ghosh, Krista Hennig, Stephanie Norton, Wen-Ning Zhao, Surya A. Reis, et al. 2011. "Short-Chain HDAC Inhibitors Differentially Affect Vertebrate Development and Neuronal Chromatin." *ACS Medicinal Chemistry Letters* 2 (1): 39–42. https://doi.org/10.1021/ml1001954.

Gaulton, Anna, Anne Hersey, Michał Nowotka, A. Patrícia Bento, Jon Chambers, David Mendez, Prudence Mutowo, et al. 2017. "The ChEMBL Database in 2017." *Nucleic Acids Research* 45 (D1): D945–54. https://doi.org/10.1093/nar/gkw1074.

Giannini, Giuseppe, Loredana Vesci, Gianfranco Battistuzzi, Davide Vignola, Ferdinando M. Milazzo, Mario Berardino Guglielmi, Marcella Barbarino, et al. 2014. "ST7612AA1, a Thioacetate-ω(γ-Lactam Carboxamide) Derivative Selected from a Novel Generation of Oral HDAC Inhibitors." *Journal of Medicinal Chemistry* 57 (20): 8358–77. https://doi.org/10.1021/jm5008209.

Goodford, P. J. 1985. "A Computational Procedure for Determining Energetically Favorable Binding Sites on Biologically Important Macromolecules." *Journal of Medicinal Chemistry* 28 (7): 849–57. https://doi.org/10.1021/jm00145a002.

Goracci, Laura, Nathalie Deschamps, Giuseppe Marco Randazzo, Charlotte Petit, Carolina Dos Santos Passos, Pierre-Alain Carrupt, Claudia Simões-Pires, and Alessandra Nurisso. 2016. "A Rational Approach for the Identification of Non-Hydroxamate HDAC6-Selective Inhibitors." *Scientific Reports* 6 (1): 29086. https://doi.org/10.1038/srep29086.

Hai, Yang, and David W. Christianson. 2016. "Histone Deacetylase 6 Structure and Molecular Basis of Catalysis and Inhibition." *Nature Chemical Biology* 12 (9): 741–47. https://doi.org/10.1038/nchembio.2134.

Hermant, Paul, Damien Bosc, Catherine Piveteau, Ronan Gealageas, Baovy Lam, Cyril Ronco, Matthieu Roignant, et al. 2017. "Controlling Plasma Stability of Hydroxamic Acids: A MedChem Toolbox." *Journal of Medicinal Chemistry* 60 (21): 9067–89. https://doi.org/10.1021/acs.jmedchem.7b01444.

Homeyer, Nadine, and Holger Gohlke. 2012. "Free Energy Calculations by the Molecular Mechanics Poisson-Boltzmann Surface Area Method." *Molecular Informatics* 31 (2): 114–22. https://doi.org/10.1002/minf.201100135.

Ibrahim Uba, Abdullahi, and Kemal Yelekçi. 2019. "Homology Modeling of Human Histone Deacetylase 10 and Design of Potential Selective Inhibitors." *Journal of Biomolecular Structure and Dynamics* 0 (0): 10. https://doi.org/10.1080/07391102.2018.1521747.

Irwin, John J., Teague Sterling, Michael M. Mysinger, Erin S. Bolstad, and Ryan G. Coleman. 2012. "ZINC: A Free Tool to Discover Chemistry for Biology." *Journal of Chemical Information and Modeling* 52 (7): 1757–68. https://doi.org/10.1021/ci3001277.

Jacobsen, Jennifer A., Jessica L. Fullagar, Melissa T. Miller, and Seth M. Cohen. 2011. "Identifying Chelators for Metalloprotein Inhibitors Using a Fragment-Based Approach." *Journal of Medicinal Chemistry* 54 (2): 591–602. https://doi.org/10.1021/jm101266s.

Jones, Gareth, Peter Willett, Robert C Glen, Andrew R Leach, and Robin Taylor. 1997. "Development and Validation of a Genetic Algorithm for Flexible Docking." *Journal of Molecular Biology* 267 (3): 727–48. https://doi.org/10.1006/JMBI.1996.0897.

Jones, Philip, Matthew J. Bottomley, Andrea Carfí, Ottavia Cecchetti, Federica Ferrigno, Paola Lo Surdo, Jesus M. Ontoria, et al. 2008. "2-Trifluoroacetylthiophenes, a Novel Series of Potent and Selective Class II Histone Deacetylase Inhibitors." *Bioorganic & Medicinal Chemistry Letters* 18 (11): 3456–61. https://doi.org/10.1016/J.BMCL.2008.02.026.

Kalin, Jay H., and Joel A. Bergman. 2013. "Development and Therapeutic Implications of Selective Histone Deacetylase 6 Inhibitors." *Journal of Medicinal Chemistry* 56 (16): 6297–6313. https://doi.org/10.1021/jm4001659.

Kashyap, Kriti, and Rita Kakkar. 2019. "An Insight into Selective and Potent Inhibition of Histone Deacetylase 8 through Induced-Fit Docking, Pharmacophore Modeling and QSAR Studies." *Journal of Biomolecular Structure and Dynamics* 0 (0): 1–18. https://doi.org/10.1080/07391102.2019.1567388.

Kawai, Kentaro, and Naoya Nagata. 2012. "Metal–Ligand Interactions: An Analysis of Zinc Binding Groups Using the Protein Data Bank." *European Journal of Medicinal Chemistry* 51 (May): 271–76. https://doi.org/10.1016/j.ejmech.2012.02.028.

Kemp, Melissa M., Qiu Wang, Jason H. Fuller, Nathan West, Nicole M. Martinez, Elizabeth M. Morse, Michel Weïwer, Stuart L. Schreiber, James E. Bradner, and Angela N. Koehler. 2011. "A Novel HDAC Inhibitor with a Hydroxy-Pyrimidine Scaffold." *Bioorganic & Medicinal Chemistry Letters* 21 (14): 4164–69. https://doi.org/10.1016/J.BMCL.2011.05.098.

KrennHrubec, Keris, Brett L. Marshall, Mark Hedglin, Eric Verdin, and Scott M. Ulrich. 2007. "Design and Evaluation of 'Linkerless' Hydroxamic Acids as Selective HDAC8 Inhibitors." *Bioorganic & Medicinal Chemistry Letters* 17 (10): 2874–78. https://doi.org/10.1016/J.BMCL.2007.02.064.

Kutil, Zsofia, Zora Novakova, Marat Meleshin, Jana Mikesova, Mike Schutkowski, and Cyril Barinka. 2017. "HDAC11 Is a Fatty-Acid Deacylase."

Lagorce, David, Olivier Sperandio, Jonathan B. Baell, Maria A. Miteva, and Bruno O. Villoutreix. 2015. "FAF-Drugs3: A Web Server for Compound Property Calculation and Chemical Library Design." *Nucleic Acids Research* 43 (W1): W200–207. https://doi.org/10.1093/nar/gkv353.

Liang, Tao, and Hao Fang. 2018. "Structure, Functions and Selective Inhibitors of HDAC6." *Current Topics in Medicinal Chemistry* 18 (28): 2429–47. https://doi.org/10.2174/1568026619666181129141822.

Lindorff-Larsen, Kresten, Stefano Piana, Kim Palmo, Paul Maragakis, John L. Klepeis, Ron O. Dror, and David E. Shaw. 2010. "Improved Side-Chain Torsion Potentials for the Amber Ff99SB Protein Force Field." *Proteins: Structure, Function and Bioinformatics* 78 (8): 1950–58. https://doi.org/10.1002/prot.22711.

M.J. Frisch, G.W. Trucks, H.B. Schlegel, G.E. Scuseria, M.A. Robb, J.R. Cheeseman, G. Scalmani, V. Barone, B. Mennucci, G.A. Petersson, H. Nakatsuji, M. Caricato, X. Li, H.P. Hratchian, A.F. Izmaylov, J. Bloino, G. Zheng, J.L. Sonnenberg, M. Hada, M. Ehar, and D.J. Fox. 2009. "Gaussian 09, Revision D.01."

Mahalakshmi, R., P. Husayn Ahmed, and Vijayalakshmi Mahadevan. 2018. "HDAC Inhibitors Show Differential Epigenetic Regulation and Cell Survival Strategies on P53 Mutant Colon Cancer Cells." *Journal of Biomolecular Structure and Dynamics* 36 (4): 938–55. https://doi.org/10.1080/07391102.2017.1302820.

Martin, David P., Patrick G. Blachly, Amy R. Marts, Tessa M. Woodruff, César A. F. de Oliveira, J. Andrew McCammon, David L. Tierney, and Seth M. Cohen. 2014. "'Unconventional' Coordination Chemistry by Metal Chelating Fragments in a

Metalloprotein Active Site." *Journal of the American Chemical Society* 136 (14): 5400–5406. https://doi.org/10.1021/ja500616m.

Martínez-Rosell, Gerard, Toni Giorgino, and Gianni De Fabritiis. 2017. "PlayMolecule ProteinPrepare: A Web Application for Protein Preparation for Molecular Dynamics Simulations." *Journal of Chemical Information and Modeling* 57 (7): 1511–16. https://doi.org/10.1021/acs.jcim.7b00190.

Mazitschek, Ralph, Vishal Patel, Dyann F. Wirth, and Jon Clardy. 2008. "Development of a Fluorescence Polarization Based Assay for Histone Deacetylase Ligand Discovery." *Bioorganic & Medicinal Chemistry Letters* 18 (9): 2809–12. https://doi.org/10.1016/J.BMCL.2008.04.007.

Morris, Garrett M., David S. Goodsell, Robert S. Halliday, Ruth Huey, William E. Hart, Richard K. Belew, and Arthur J. Olson. 1998. "Automated Docking Using a Lamarckian Genetic Algorithm and an Empirical Binding Free Energy Function." *Journal of Computational Chemistry* 19 (14): 1639–62. https://doi.org/10.1002/(SICI)1096-987X(19981115)19:14<1639::AID-JCC10>3.0.CO;2-B.

Murray-Thompson, Monique, Zining Wu, Robert A Reid, Dulce Soler, Michael A Nolan, Quentin G Wright, Mary B Moyer, et al. 2013. "Selective Class IIa Histone Deacetylase Inhibition via a Nonchelating Zinc-Binding Group." *Nature Chemical Biology* 9 (5): 319–25. https://doi.org/10.1038/nchembio.1223.

Muthyala, Ramaiah, Woo Shik Shin, Jiashu Xie, and Yuk Yin Sham. 2015. "Discovery of 1-Hydroxypyridine-2-Thiones as Selective Histone Deacetylase Inhibitors and Their Potential Application for Treating Leukemia." *Bioorganic & Medicinal Chemistry Letters* 25 (19): 4320–24. https://doi.org/10.1016/J.BMCL.2015.07.065.

Olson, David E., Florence F. Wagner, Taner Kaya, Jennifer P. Gale, Nadia Aidoud, Emeline L. Davoine, Fanny Lazzaro, Michel Weïwer, Yan-Ling Zhang, and Edward B. Holson. 2013. "Discovery of the First Histone Deacetylase 6/8 Dual Inhibitors." *Journal of Medicinal Chemistry* 56 (11): 4816–20. https://doi.org/10.1021/jm400390r.

Otava Chemicals. 2017. "Otava Chelator Fragment Library." http://www.otavachemicals.com/.

Paissoni, C., D. Spiliotopoulos, G. Musco, and A. Spitaleri. 2015. "GMXPBSA 2.1: A GROMACS Tool to Perform MM/PBSA and Computational Alanine Scanning." *Computer Physics Communications* 186 (January): 105–7. https://doi.org/10.1016/J.CPC.2014.09.010.

Pande, Vineet. 2016. "Understanding the Complexity of Epigenetic Target Space." *Journal of Medicinal Chemistry* 59 (4): 1299–1307. https://doi.org/10.1021/acs.jmedchem.5b01507.

Patil, Vishal, Quaovi H. Sodji, James R. Kornacki, Milan Mrksich, and Adegboyega K. Oyelere. 2013. "3-Hydroxypyridin-2-Thione as Novel Zinc Binding Group for Selective Histone Deacetylase Inhibition." *Journal of Medicinal Chemistry* 56 (9): 3492–3506. https://doi.org/10.1021/jm301769u.

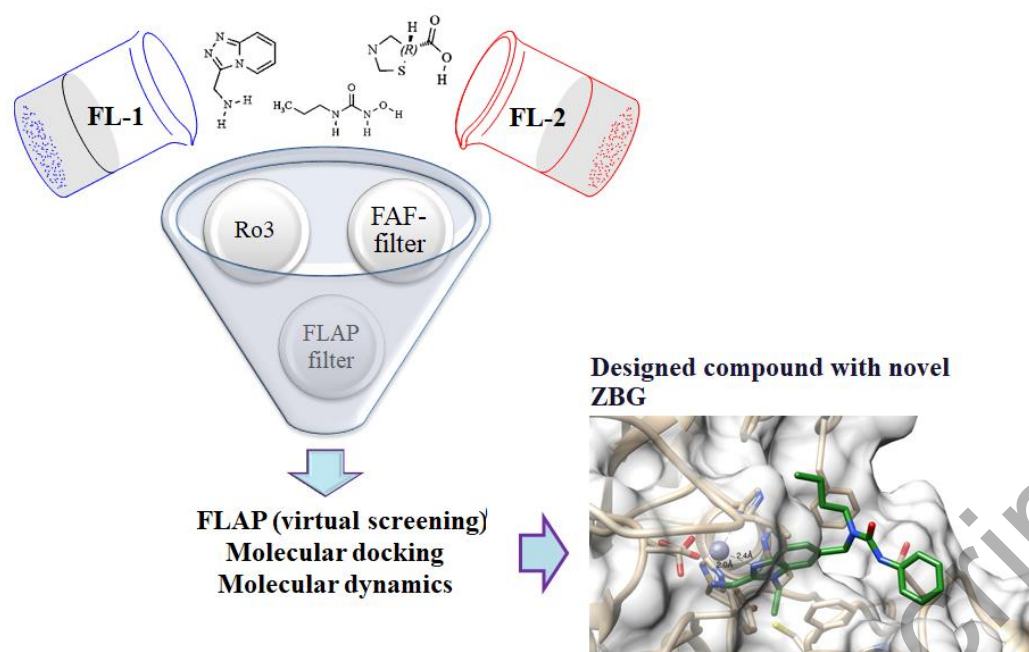PerkinElmer. 2015. "ChemDraw - Chemical Drawing Software | PerkinElmer." http://www.perkinelmer.com/category/chemdraw.

Perruccio, Francesca, Jonathan S. Mason, Simone Sciabola, and Massimo Baroni. 2006. "FLAP: 4-Point Pharmacophore Fingerprints from GRID." In *Molecular Interaction Fields: Applications in Drug Discovery and ADME Prediction*, 27:83–102. John Wiley & Sons, Ltd. https://doi.org/10.1002/3527607676.ch4.

Porter, Nicholas J., Adaickapillai Mahendran, Ronald Breslow, and David W. Christianson. 2017. "Unusual Zinc-Binding Mode of HDAC6-Selective Hydroxamate Inhibitors." *Proceedings of the National Academy of Sciences* 114 (51): 13459–64. https://doi.org/10.1073/pnas.1718823114.

Porter, Nicholas J., Jeremy D. Osko, Daniela Diedrich, Thomas Kurz, Jacob M. Hooker, Finn K. Hansen, and David W. Christianson. 2018. "Histone Deacetylase 6-Selective Inhibitors and the Influence of Capping Groups on Hydroxamate-Zinc Denticity." *Journal of Medicinal Chemistry* 61 (17): 8054–60. https://doi.org/10.1021/acs.jmedchem.8b01013.

Porter, Nicholas J., Florence F. Wagner, and David W. Christianson. 2018. "Entropy as a Driver of Selectivity for Inhibitor Binding to Histone Deacetylase 6." *Biochemistry* 57 (26): 3916–24. https://doi.org/10.1021/acs.biochem.8b00367.

Pronk, Sander, Szilárd Páll, Roland Schulz, Per Larsson, Pär Bjelkmar, Rossen Apostolov, Michael R. Shirts, et al. 2013. "GROMACS 4.5: A High-Throughput and Highly Parallel Open Source Molecular Simulation Toolkit." *Bioinformatics* 29 (7): 845–54. https://doi.org/10.1093/bioinformatics/btt055.

Roche, Joëlle, and Philippe Bertrand. 2016. "Inside HDACs with More Selective HDAC Inhibitors." *European Journal of Medicinal Chemistry* 121: 451–83. https://doi.org/10.1016/j.ejmech.2016.05.047.

Ruijter, Annemieke J M de, Albert H van Gennip, Huib N Caron, Stephan Kemp, and André B P van Kuilenburg. 2003. "Histone Deacetylases (HDACs): Characterization of the Classical HDAC Family." *The Biochemical Journal* 370 (Pt 3): 737–49. https://doi.org/10.1042/BJ20021321.

Seidel, Carole, Michael Schnekenburger, Mario Dicato, and Marc Diederich. 2015. "Histone Deacetylase 6 in Health and Disease." *Epigenomics* 7 (1): 103–18. https://doi.org/10.2217/epi.14.69.

Sharma, Monika, Prakash Jha, Priyanka Verma, and Madhu Chopra. 2019. "Combined Comparative Molecular Field Analysis, Comparative Molecular Similarity Indices Analysis, Molecular Docking and Molecular Dynamics Studies of Histone Deacetylase 6 Inhibitors." *Chemical Biology and Drug Design* 93 (5): 910–25. https://doi.org/10.1111/cbdd.13488.

Shen, Sida, and Alan P. Kozikowski. 2016. "Why Hydroxamates May Not Be the Best Histone Deacetylase Inhibitors - What Some May Have Forgotten or Would Rather Forget?" *ChemMedChem* 11 (1): 15–21. https://doi.org/10.1002/cmdc.201500486.

Sixto-López, Yudibeth, Martiniano Bello, and José Correa-Basurto. 2019a. "Insights into Structural Features of HDAC1 and Its Selectivity Inhibition Elucidated by Molecular Dynamic Simulation and Molecular Docking." *Journal of Biomolecular Structure and Dynamics* 37 (3): 584–610. https://doi.org/10.1080/07391102.2018.1441072.

———. 2019b. "Structural and Energetic Basis for the Inhibitory Selectivity of Both

Catalytic Domains of Dimeric HDAC6." *Journal of Biomolecular Structure and Dynamics* 0 (0): 1–20. https://doi.org/10.1080/07391102.2018.1557560.

Søndergaard, Chresten R., Mats H.M. Olsson, Michał Rostkowski, and Jan H. Jensen. 2011. "Improved Treatment of Ligands and Coupling Effects in Empirical Calculation and Rationalization of p K a Values." *Journal of Chemical Theory and Computation* 7 (7): 2284–95. https://doi.org/10.1021/ct200133y.

Sousa da Silva, Alan W, and Wim F Vranken. 2012. "ACPYPE - AnteChamber PYthon Parser InterfacE." *BMC Research Notes* 5 (1): 367. https://doi.org/10.1186/1756-0500-5-367.

Uba, Abdullahi Ibrahim, and Kemal Yelekçi. 2018. "Identification of Potential Isoform-Selective Histone Deacetylase Inhibitors for Cancer Therapy: A Combined Approach of Structure-Based Virtual Screening, Admet Prediction and Molecular Dynamics Simulation Assay." *Journal of Biomolecular Structure and Dynamics* 36 (12): 3231–45. https://doi.org/10.1080/07391102.2017.1384402.

VanHeyst, Michael D., Sophia N. Ononye, Dennis L. Wright, Mohamed Ammar, Amy C. Anderson, Wangda Zhou, and E. Zachary Oblak. 2013. "Tropolones As Lead-Like Natural Products: The Development of Potent and Selective Histone Deacetylase Inhibitors." *ACS Medicinal Chemistry Letters* 4 (8): 757–61. https://doi.org/10.1021/ml400158k.

Vassetti, Dario, Marco Pagliai, and Piero Procacci. 2019. "Assessment of GAFF2 and OPLS-AA General Force Fields in Combination with the Water Models TIP3P, SPCE, and OPC3 for the Solvation Free Energy of Druglike Organic Molecules." Research-article. *Journal of Chemical Theory and Computation* 15 (3): 1983–95. https://doi.org/10.1021/acs.jctc.8b01039.

Wagner, Florence F., David E. Olson, Jennifer P. Gale, Taner Kaya, Michel Weïwer, Nadia Aidoud, Méryl Thomas, et al. 2013. "Potent and Selective Inhibition of Histone Deacetylase 6 (HDAC6) Does Not Require a Surface-Binding Motif." https://doi.org/10.1021/JM301355J.

Wagner, Florence F, Morten Lundh, Taner Kaya, Patrick Mccarren, Yan-ling Zhang, Shrikanta Chattopadhyay, Jennifer P Gale, et al. 2016. "An Isochemogenic Set of Inhibitors To De Fi Ne the Therapeutic Potential of Histone Deacetylases in β‐Cell Protection." https://doi.org/10.1021/acschembio.5b00640.

Wang, Xiu Xiu, Ren Zhong Wan, and Zhao Peng Liu. 2018. "Recent Advances in the Discovery of Potent and Selective HDAC6 Inhibitors." *European Journal of Medicinal Chemistry* 143: 1406–18. https://doi.org/10.1016/j.ejmech.2017.10.040.

Wang, Yijun, Limei Yang, Jiaying Hou, Qing Zou, Qi Gao, Wenhui Yao, Qizheng Yao, and Ji Zhang. 2019. "Hierarchical Virtual Screening of the Dual MMP-2/HDAC-6 Inhibitors from Natural Products Based on Pharmacophore Models and Molecular Docking." *Journal of Biomolecular Structure and Dynamics* 37 (3): 649–70. https://doi.org/10.1080/07391102.2018.1434833.

Watson, Peter J, Christopher J Millard, Andrew M Riley, Naomi S Robertson, Lyndsey C Wright, Himali Y Godage, Shaun M Cowley, Andrew G Jamieson, Barry V L Potter, and John W R Schwabe. 2016. "ARTICLE Insights into the Activation Mechanism of Class I HDAC Complexes by Inositol Phosphates."

https://doi.org/10.1038/ncomms11262.

Whitehead, Lewis, Markus R. Dobler, Branko Radetich, Yanyi Zhu, Peter W. Atadja, Tavina Claiborne, Jonathan E. Grob, et al. 2011. "Human HDAC Isoform Selectivity Achieved via Exploitation of the Acetate Release Channel with Structurally Unique Small Molecule Inhibitors." *Bioorganic and Medicinal Chemistry* 19 (15): 4626–34. https://doi.org/10.1016/j.bmc.2011.06.030.

Wu, Jianghong, Adeboye Adejare, Jeffrey Wang, Jason Wallach, Stephanie Duane, Haiching Ma, Yuren Wang, and Yuan Wang. 2017. "Developing Selective Histone Deacetylases (HDACs) Inhibitors through Ebselen and Analogs." *Drug Design, Development and Therapy* Volume 11: 1369–82. https://doi.org/10.2147/dddt.s124977.

Yang, Min, Robert Orlowski, Parameswaran Hari, Simon S Jones, Robert J Markelewicz, Noopur Raje, Jeffrey G Supko, et al. 2017. "Ricolinostat, the First Selective Histone Deacetylase 6 Inhibitor, in Combination with Bortezomib and Dexamethasone for Relapsed or Refractory Multiple Myeloma." *Clinical Cancer Research* 23 (13): 3307–15. https://doi.org/10.1158/1078-0432.ccr-16-2526.

Yuan, Yuan, Zongyue Hu, Minyue Bao, Rong Sun, Xin Long, Li Long, Jianzong Li, Chuanfang Wu, and Jinku Bao. 2018. "Screening of Novel Histone Deacetylase 7 Inhibitors through Molecular Docking Followed by a Combination of Molecular Dynamics Simulations and Ligand-Based Approach." *Journal of Biomolecular Structure and Dynamics* 0 (0): 1–12. https://doi.org/10.1080/07391102.2018.1541141.

Zhou, Hao, Chengzhang Wang, Tao Deng, Ran Tao, and Wenjun Li. 2018. "Novel Urushiol Derivatives as HDAC8 Inhibitors: Rational Design, Virtual Screening, Molecular Docking and Molecular Dynamics Studies." *Journal of Biomolecular Structure and Dynamics* 36 (8): 1966–78. https://doi.org/10.1080/07391102.2017.1344568.

Graphical Abstract

Designed compound with novel ZBG

FL-1   FL-2

Ro3   FAF-filter

FLAP filter

FLAP (virtual screening)
Molecular docking
Molecular dynamics